

Sep 02, 2021

## 3.1 Synthesis of Glutathione Beads

✓ Book Chapter

📁 In 1 collection

Peter Simons<sup>1</sup>, Virginie Bondu<sup>1</sup>, Angela Wandinger-Ness<sup>1</sup>, Tione Buranda<sup>1</sup><sup>1</sup>Department of Pathology, University of New Mexico School of Medicine, Albuquerque, USA

1 Works for me

🔗 Share

[dx.doi.org/10.17504/protocols.io.bptqnmnw](https://dx.doi.org/10.17504/protocols.io.bptqnmnw)

Springer Nature Books

satyavati Kharde

### ABSTRACT

Small, monomeric guanine triphosphate hydrolases (GTPases) are ubiquitous cellular integrators of signaling. A signal activates the GTPase, which then binds to an effector molecule to relay a signal inside the cell. The GTPase effector trap flow cytometry assay (G-Trap) utilizes bead-based protein immobilization and dual-color flow cytometry to rapidly and quantitatively measure GTPase activity status in cell or tissue lysates. Beginning with commercial cytoflex bead sets that are color-coded with graded fluorescence intensities of a red (700 nm) wavelength, the bead sets are derivatized to display glutathione on the surface through a detailed protocol described here. A different glutathione-S-transferase-effector protein (GST-effector protein) can then be attached to the surface of each set. For the assay, users can incubate bead sets individually or in a multiplex format with lysates for rapid, selective capture of active, GTP-bound GTPases from a single sample. After that, flow cytometry is used to identify the bead-borne GTPase based on red bead intensity, and the amount of active GTPase per bead is detected using monoclonal antibodies conjugated to a green fluorophore or via labeled secondary antibodies. Three examples are provided to illustrate the efficacy of the effector-functionalized beads for measuring the activation of at least five GTPases in a single lysate from fewer than 50,000 cells.

Section 3.1 'Synthesis of Glutathione Beads' from 'Small-Volume Flow Cytometry-Based Multiplex Analysis of the Activity of Small GTPases' <https://www.protocols.io/view/small-volume-flow-cytometry-based-multiplex-analysis-bpssmnee>

DOI

[dx.doi.org/10.17504/protocols.io.bptqnmnw](https://dx.doi.org/10.17504/protocols.io.bptqnmnw)

EXTERNAL LINK

[https://link.springer.com/protocol/10.1007/978-1-4939-8612-5\\_13](https://link.springer.com/protocol/10.1007/978-1-4939-8612-5_13)

PROTOCOL CITATION

Peter Simons, Virginie Bondu, Angela Wandinger-Ness, Tione Buranda 2021. 3.1 Synthesis of Glutathione Beads. **protocols.io**  
<https://dx.doi.org/10.17504/protocols.io.bptqnmnw>

MANUSCRIPT CITATION please remember to cite the following publication along with this protocol

Simons P., Bondu V., Wandinger-Ness A., Buranda T. (2018) Small-Volume Flow Cytometry-Based Multiplex Analysis of the Activity of Small GTPases. In: Rivero F. (eds) Rho GTPases. Methods in Molecular Biology, vol 1821. Humana Press, New York, NY. [https://doi.org/10.1007/978-1-4939-8612-5\\_13](https://doi.org/10.1007/978-1-4939-8612-5_13)

COLLECTIONS ⓘ

 **Small-Volume Flow Cytometry-Based Multiplex Analysis of the Activity of Small GTPases**

## KEYWORDS

Rho GTPase, Rab GTPase, Cell signaling, Cytoskeleton, Hantavirus, Flow cytometry, Integrin activation, Sepsis, Multiplex, Protease-activated receptors, PARs, Thrombin, Argatroban, Bead functionalization, Glutathione-S-transferase, GST, GTPase effector beads, Rap1, RhoA, Rac1, Rab7, Fluorescence calibration beads

## LICENSE

————— This is an open access protocol distributed under the terms of the [Creative Commons Attribution License](#), which permits unrestricted use, distribution, and reproduction in any medium, provided the original author and source are credited

## CREATED

Nov 17, 2020

## LAST MODIFIED

Sep 02, 2021

## OWNERSHIP HISTORY

Nov 17, 2020  Lenny Teytelman protocols.io

Jul 05, 2021  Emma Ganley protocols.io

Aug 24, 2021  Satyavati Kharde

Aug 26, 2021  satyavati Kharde

## PROTOCOL INTEGER ID

44624

## PARENT PROTOCOLS

Part of collection

[Small-Volume Flow Cytometry-Based Multiplex Analysis of the Activity of Small GTPases](#)

## GUIDELINES

## Introduction

Members of the Ras-related superfamily of small, monomeric GTPases, including Rho, Ras, and Rab subfamilies, serve as critical integrators of cellular functions from cell division and survival to membrane trafficking [1-6]. Genetic diseases and infectious agents such as viruses and bacteria are known to co-opt the signaling functions of GTPases, making GTPases attractive diagnostic and therapeutic targets [7-15]. Current methods for measuring the activation status of small GTPases rely on glutathione bead-based effector pull-down/immunoblot assays, and ELISA-based effector-binding assay kits. The significant shortcomings of these methods are that they are labor intensive and require large sample sizes, purified effector proteins, or expensive kits. Additionally, sample processing times are critical because of the lability of the GTP-bound state due to hydrolysis. Here we describe the GTPase activity assay platform (G-Trap) [16], a multiplex, bead-based effector-binding assay that can rapidly monitor the activation status of multiple GTPases from a single-cell lysate [16, 17].

The GST-effector proteins consisting of the minimal GTPase-binding domains (RBD) for the studies are PAK-1 RBD (a Rac1 and Cdc42 effector), Raf-1 RBD (a Ras effector), Rhotekin-RBD (a Rho effector), RalGDS-RBD (a RAP1 effector protein), and RILP-RBD (a Rab7 effector) [16, 17]. Beads for each target effector (10,000/target) are mixed and added to cell lysates typically generated from 50,000 cells. The beads are incubated with cell lysates for 1 h at 4 °C, centrifuged, and resuspended in 50 µL of buffer (1:20 final antibody dilution). Monoclonal antibodies for each target GTPase are pooled and added to the multiplex bead suspension and incubated for 1 h at 4 °C. A secondary antibody tagged with Alexa 488 dye is then used to label bead-associated antibodies fluorescently. The samples are then analyzed on a flow cytometer where the red fluorescence identifies the specific effector bead and is used to gate the green fluorescence and quantify the amount of each target, GTP-bound GTPase. We

demonstrate the functionality of the assay in three tests involving the activation of multiple GTPases. The first example measures the signaling cascade of GTPases that are activated to allow  $\beta_3$  integrin-mediated cellular entry of Sin Nombre virus (SNV) in the course of a productive infection [16, 17]. The second example measures GTPase activity downstream of signaling of protease-activated receptors (PARs), after exposure to thrombin found in the plasma samples drawn from patients with hantavirus cardiopulmonary syndrome (HCPS) [18]. The third example measures GTPase activation due to bacterial factors [12, 19] present in a plasma sample from a septic patient. Control reagents used for these illustrative examples are given in Table 1.

A	B	C	D	E
GTPase	Effector	Activator; final concentration; incubation time	Inhibitor; final concentration; incubation time	SNV particle titer; incubation time
RhoA	Rhotekin RBD	Calpeptin; 1 $\mu$ M; 30 min		10,000/cell; 3, 10, 20, 30, 60 min
Rac1	PAK-1 PBD	EGF; 10 nM; 15 min	NSC23766; 100 $\mu$ M; 30 min	10,000/cell; 3, 10, 20, 30, 60 min
Rap1	Ral-GDS RBD	8-Cpt-2me-cAMP; 50 $\mu$ M; 30 min	GGTI 298; 10 $\mu$ M; 30 min	10,000/cell; 3, 10, 20, 30, 60 min
R-Ras	Raf-1 RBD		FTI-277; 100 nM; 30 min	
H-Ras	Raf-1 RBD		FTI-277; 100 nM; 30 min	
Rab7	RILP RBD	EGF; 10 nM; 15 min		10,000/cell; 3, 10, 20, 30, 60 min

Table 1 Reagents, concentrations, and conditions used for illustrative experiments [16]

It is well established that flow cytometry is an ideal platform for measuring multiple analytes, simultaneously using cytoflex bead populations encoded with fluorescent dyes of graded intensities, with which the bead is uniquely identified (*see* Fig. 1) [17, 20]. Flow cytometry is capable of exciting at multiple absorption bands and detecting fluorescence at different emission wavelengths, and it is then possible to detect various analytes, simultaneously from a single sample [21-25]. The commercially available cytoflex beads used by us have up to 12 different intensity levels that can be used as unique bead identifiers. Furthermore, the beads are currently available in two sizes that can be resolved by flow cytometry forward light scatter. Thus, up to 24 different analytes can be measured. Our experience to date suggests that a maximum of six targets at a time is optimal for reproducible assay results [17].

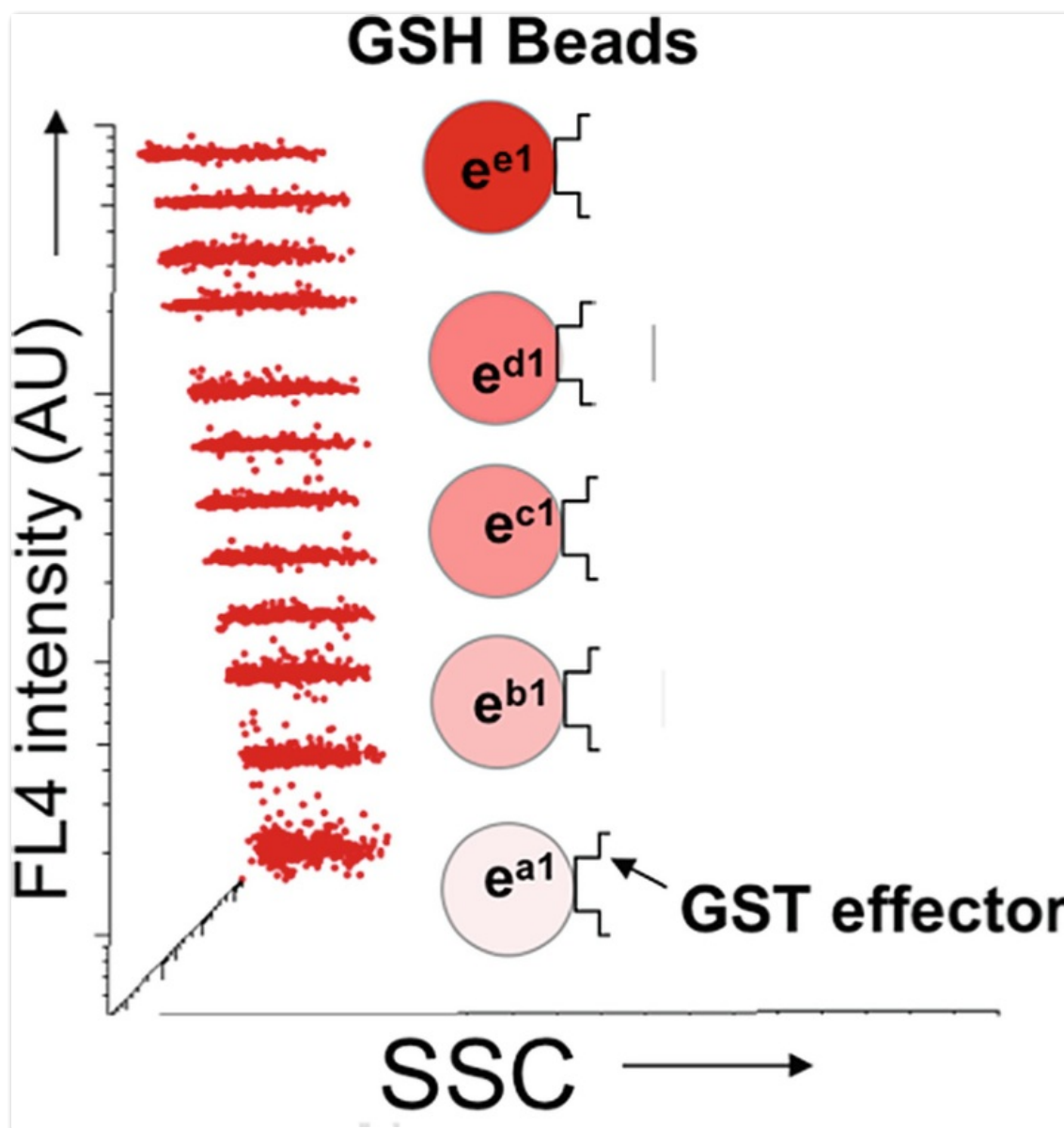


Fig. 1

The GTPase effector trap flow cytometry assay (G-Trap). The plot of red fluorescence (FL4) versus side scatter (SSC) of a set of 12 of Cyto-Plex™ beads dyed with 12 discrete levels of 700 nm fluorescence. In the G-Trap assay, the letters *a*, *b*, *c*, *d*, and *e* identify and link effectors, their cognate GTPases, and fluorescently labeled antibodies FL1 (520 nm emission) or FL2 (580 nm emission) used for readout. In single or multiplex format, glutathione bead populations coated with effectors are used to capture specific active GTPases. In multiplex format, the effector and GTPase identities are defined by the intensity level of red fluorescence encoded on each bead

## Notes

1. The site density of glutathione sites on beads governs the magnitude of the fluorescence signal from GST proteins bound to the beads. A low site density of GST sites on beads can yield variable data or poor binding results [28]. Derivatization of the carboxyl Cyto-Plex™ beads to glutathione requires an intermediate step of functionalizing to amino groups. Optimizing the synthesis of amino groups is essential. Derivatizing the amino-terminated groups with a fluorescent probe such as NHS-Alexa 488 tests optimum conversion of carboxyl to amino groups. For this purpose, it is useful to use inexpensive carboxyl-functionalized beads such as those from SpheroTech (see **Note 3**). Glutathione derivatization is tested with 25 nM GST-GFP for 30 min as described in the note in **step 14**.

2. All buffers contain 0.01% Tween-20, which is compatible with most biological molecules.

3. To test the conversion efficiency of carboxyl beads to amino beads, we derivatized 10  $\mu$ L of generic carboxyl beads (Spherotech) to amino beads. We use commercial amino beads of similar size with known amino group site density for comparison, with our synthesis. The two amino bead sets are then reacted with NHS-Alexa488 in parallel. Approximately 0.1 mg of NHS-Alexa488 is dissolved in 20  $\mu$ L of dry DMSO to give about 5 mg/mL, which is stored at  $-80^{\circ}\text{C}$ . Ten thousand synthesized amino beads and ten thousand commercial amino beads are put in 20  $\mu$ L of pH 8.4 buffer, 2  $\mu$ L of NHS-Alexa488 solution is added, the suspension is mixed, and reagents are allowed to react for 30 min in the dark. The beads are washed twice with pH 7 buffer, diluted to 50  $\mu$ L of buffer, and analyzed by flow cytometry. We determine nonspecific binding of NHS-Alexa488 to beads by mixing carboxyl beads with the fluorophore. In our setting the fluorescence from the nonspecific attachment of NHS-Alexa488 to carboxyl beads was 20% of the conjugated fluorophores. Our amino beads were comparable to the commercial beads.

4. Bubbling nitrogen slowly through 400  $\mu$ L of suspension in a 1.6 mL microfuge tube is not easy. We use a narrow nitrogen line and very low nitrogen pressure, and notice that the angle of the tube of suspended beads matters: tipping the slowly bubbling microfuge tube from horizontal to upright can stop bubbling, probably due to increased hydrostatic pressure. Another technique to prevent bubbling is to use a soft nitrogen tubing line, which can be pushed against the bottom of the centrifuge tube to stop bubbling. Tween-20 gives an observable bubble running up the microfuge tube, and we estimate that the volume of air above the suspension is displaced about ten times during the 2 min of bubbling.

5. Blocking of nonspecific binding sites for primary and secondary antibodies with BSA is critical for limiting nonspecific binding. It is also important to test new antibodies in single-target format before using in a multiplex format. In our experience new antibody batches from “trusted sources” can be highly nonspecific, and could bind to all bead surfaces regardless of effector functionalization, and either raise the background intensity for all beads in the multiplex assay or at worst degrade the readout of all the beads in a multiplex configuration.

## Acknowledgments

This work was supported by National Institutes of Health (NIH) grants R03AI092130 and R21NS066429 to TB; NIH R21 NS066435, NSF MCB0956027, and DOD OC110514 to AWN; and NSF I-Corps 7775897 to AWN and TB.

## References

1. Jaffe AB, Hall A (2005) Rho GTPases: biochemistry and biology. *Annu Rev Cell Dev Biol* 21:247–269 [CrossRef](#) [Google Scholar](#)
2. Ridley A (2000) Rho GTPases. Integrating integrin signaling. *J Cell Biol* 150:F107–F109 [CrossRef](#) [PubMed](#) [PubMedCentral](#) [Google Scholar](#)
3. Bar-Sagi D, Hall A (2000) Ras and Rho GTPases: a family reunion. *Cell* 103:227–238 [CrossRef](#) [PubMed](#) [Google Scholar](#)
4. Van Aelst L, D'Souza-Schorey C (1997) Rho GTPases and signaling networks. *Genes Dev* 11:2295–2322 [CrossRef](#) [PubMed](#) [Google Scholar](#)
5. Nobes C, Hall A (1994) Regulation and function of the Rho subfamily of small GTPases. *Curr Opin Genet Dev* 4:77–81 [CrossRef](#) [PubMed](#) [Google Scholar](#)
6. Vega FM, Ridley AJ (2007) SnapShot: Rho family GTPases. *Cell* 129:1430 [CrossRef](#) [PubMed](#) [Google Scholar](#)
7. Hong L, Kenney SR, Phillips GK, Simpson D, Schroeder CE, Noth J, Romero E, Swanson S, Waller A, Strouse JJ, Carter M, Chigaev A, Ursu O, Oprea T, Hjelle B, Golden JE, Aube J, Hudson LG, Buranda T, Sklar LA, Wandinger-Ness A (2013) Characterization of a cdc42 protein inhibitor and its use as a molecular probe. *J Biol Chem* 288:8531–8543 [CrossRef](#) [PubMed](#) [PubMedCentral](#) [Google Scholar](#)
8. Agola JO, Hong L, Surviladze Z, Ursu O, Waller A, Strouse JJ, Simpson DS, Schroeder CE, Oprea TI, Golden JE, Aube J, Buranda T, Sklar LA, Wandinger-Ness A (2012) A competitive nucleotide binding inhibitor: in vitro characterization of Rab7 GTPase inhibition. *ACS Chem Biol* 7:1095–1108 [CrossRef](#) [PubMed](#) [PubMedCentral](#) [Google Scholar](#)
9. Friesland A, Zhao Y, Chen YH, Wang L, Zhou H, Lu Q (2013) Small molecule targeting Cdc42-intersectin interaction disrupts Golgi organization and suppresses cell motility. *Proc Natl Acad Sci U S A* 110:1261–1266 [CrossRef](#) [PubMed](#) [PubMedCentral](#) [Google Scholar](#)
10. Vega FM, Ridley AJ (2008) Rho GTPases in cancer cell biology. *FEBS Lett* 582:2093–2101 [CrossRef](#) [Google](#)

## Scholar

11. Boyer L, Lemichez E (2015) Switching Rho GTPase activation into effective antibacterial defenses requires the caspase-1/IL-1 $\beta$  signaling axis. *Small GTPases* 6:186–188 [CrossRef](#) [PubMed](#) [PubMedCentral](#) [Google Scholar](#)
12. Lemichez E, Aktories K (2013) Hijacking of Rho GTPases during bacterial infection. *Exp Cell Res* 319:2329–2336 [CrossRef](#) [PubMed](#) [Google Scholar](#)
13. Agola JO, Sivalingam D, Cimino DF, Simons PC, Buranda T, Sklar LA, Wandinger-Ness A (2015) Quantitative bead-based flow cytometry for assaying Rab7 GTPase interaction with the Rab-interacting lysosomal protein (RILP) effector protein. *Methods Mol Biol* 1298:331–354 [CrossRef](#) [PubMed](#) [PubMedCentral](#) [Google Scholar](#)
14. Guo Y, Kenney SR, Cook L, Adams SF, Rutledge T, Romero E, Oprea TI, Sklar LA, Bedrick E, Wiggins CL, Kang H, Lomo L, Muller CY, Wandinger-Ness A, Hudson LG (2015) A novel pharmacologic activity of ketorolac for therapeutic benefit in ovarian cancer patients. *Clin Cancer Res* 21:5064–5072 [CrossRef](#) [PubMed](#) [PubMedCentral](#) [Google Scholar](#)
15. Guo Y, Kenney SR, Muller CY, Adams S, Rutledge T, Romero E, Murray-Krezaan C, Prekeris R, Sklar LA, Hudson LG, and Wandinger-Ness A (2015) R-Ketorolac targets Cdc42 and Rac1 and alters ovarian cancer cell behaviors critical for invasion and metastasis. *Mol Cancer Ther* 14:2215–2227 [CrossRef](#) [PubMed](#) [PubMedCentral](#) [Google Scholar](#)
16. Buranda T, Basuray S, Swanson S, Bondu-Hawkins V, Agola J, Wandinger-Ness A (2013) Rapid parallel flow cytometry assays of active GTPases using effector beads. *Anal Biochem* 444:149–157 [CrossRef](#) [Google Scholar](#)
17. Bondu V, Wu C, Cao W, Simons PC, Gillette JM, Zhu J, Erb L, Zhang XF, Buranda T (2017) Low affinity binding in cis to P2Y2R mediates force-dependent integrin activation during hantavirus infection. *Mol Biol Cell* 28:2887–2903 [CrossRef](#) [PubMed](#) [PubMedCentral](#) [Google Scholar](#)
18. Bondu V, Schrader R, Gawinowicz MA, McGuire P, Lawrence DA, Hjelle B, Buranda T (2015) Elevated cytokines, thrombin and PAI-1 in severe HCPS patients due to Sin Nombre virus. *Virus* 7:559–589 [CrossRef](#) [Google Scholar](#)
19. Boquet P, Lemichez E (2003) Bacterial virulence factors targeting Rho GTPases: parasitism or symbiosis? *Trends Cell Biol* 13:238–246 [CrossRef](#) [PubMed](#) [Google Scholar](#)
20. Curpan RF, Simons PC, Zhai D, Young SM, Carter MB, Bologa CG, Oprea TI, Satterthwait AC, Reed JC, Edwards BS, Sklar LA (2011) High-throughput screen for the chemical inhibitors of antiapoptotic bcl-2 family proteins by multiplex flow cytometry. *Assay Drug Dev Technol* 9:465–474 [CrossRef](#) [PubMed](#) [PubMedCentral](#) [Google Scholar](#)
21. Buican TN, Hoffmann GW (1985) Immunofluorescent flow cytometry in N dimensions. The multiplex labeling approach. *Cell Biophys* 7:129–156 [CrossRef](#) [PubMed](#) [Google Scholar](#)
22. Camp CH Jr, Yegnanarayanan S, Eftekhari AA, Adibi A (2011) Label-free flow cytometry using multiplex coherent anti-Stokes Raman scattering (MCARS) for the analysis of biological specimens. *Opt Lett* 36:2309–2311 [CrossRef](#) [PubMed](#) [Google Scholar](#)
23. Davies R, Vogelsang P, Jonsson R, Appel S (2016) An optimized multiplex flow cytometry protocol for the analysis of intracellular signaling in peripheral blood mononuclear cells. *J Immunol Methods* 436:58–63 [CrossRef](#) [PubMed](#) [Google Scholar](#)
24. Merat SJ, van de Berg D, Bru C, Yasuda E, Breij E, Kooststra N, Prins M, Molenkamp R, Bakker AQ, de Jong MD, Spits H, Schinkel J, Beaumont T (2017) Multiplex flow cytometry-based assay to study the breadth of antibody responses against E1E2 glycoproteins of hepatitis C virus. *J Immunol Methods* 454:15–26. <https://doi.org/10.1016/j.jim.2017.07.015> [CrossRef](#) [PubMed](#) [Google Scholar](#)
25. Saunders MJ, Graves SW, Sklar LA, Oprea TI, Edwards BS (2010) High-throughput multiplex flow cytometry screening for botulinum neurotoxin type A light chain protease inhibitors. *Assay Drug Dev Technol* 8:37–46 [CrossRef](#) [PubMed](#) [PubMedCentral](#) [Google Scholar](#)
26. Tessema M, Simons PC, Cimino DF, Sanchez L, Waller A, Posner RG, Wandinger-Ness A, Prossnitz ER, Sklar LA (2006) Glutathione-S-transferase-green fluorescent protein fusion protein reveals slow dissociation from high site density beads and measures free GSH. *Cytometry A* 69:326–334 [CrossRef](#) [PubMed](#) [Google Scholar](#)
27. Schwartz SL, Tessema M, Buranda T, Pylypenko O, Rak A, Simons PC, Surviladze Z, Sklar LA, Wandinger-Ness A (2008) Flow cytometry for real-time measurement of guanine nucleotide binding and exchange by Ras-like GTPases. *Anal Biochem* 381:258–266 [CrossRef](#) [PubMed](#) [PubMedCentral](#) [Google Scholar](#)
28. Surviladze Z, Young SM, Sklar LA (2012) High-throughput flow cytometry bead-based multiplex assay for identification of Rho GTPase inhibitors. *Methods Mol Biol* 827:253–270 [CrossRef](#) [PubMed](#) [PubMedCentral](#) [Google Scholar](#)
29. Buranda T, Swanson S, Bondu V, Schaefer L, Maclean J, Mo ZZ, Wycoff K, Belle A, Hjelle B (2014) Equilibrium and kinetics of Sin Nombre hantavirus binding at DAF/CD55 functionalized bead surfaces. *Virus* 6:1091–1111 [CrossRef](#) [Google Scholar](#)
30. Buranda T, Wu Y, Sklar LA (2011) Quantum dots for quantitative flow cytometry. *Methods Mol Biol* 699:67–84 [CrossRef](#) [PubMed](#) [PubMedCentral](#) [Google Scholar](#)
31. Buranda T, Jones GM, Nolan JP, Keij J, Lopez GP, Sklar LA (1999) Ligand receptor dynamics at streptavidin-



- coated particle surfaces: a flow cytometric and spectrofluorimetric study. *J Phys Chem B* 29:3399–3410 [CrossRef](#) [Google Scholar](#)
32. Shen B, Delaney MK, Du X (2012) Inside-out, outside-in, and inside-outside-in: G protein signaling in integrin-mediated cell adhesion, spreading, and retraction. *Curr Opin Cell Biol* 24:600–606 [CrossRef](#) [PubMed](#) [PubMedCentral](#) [Google Scholar](#)
  33. Springer TA, Dustin ML (2012) Integrin inside-out signaling and the immunological synapse. *Curr Opin Cell Biol* 24:107–115 [CrossRef](#) [PubMed](#) [Google Scholar](#)
  34. Nordenfelt P, Elliott HL, Springer TA (2016) Coordinated integrin activation by actin-dependent force during T-cell migration. *Nat Commun* 7:13119 [CrossRef](#) [PubMed](#) [PubMedCentral](#) [Google Scholar](#)
  35. Schurpf T, Springer TA (2011) Regulation of integrin affinity on cell surfaces. *EMBO J* 30:4712–4727 [CrossRef](#) [PubMed](#) [PubMedCentral](#) [Google Scholar](#)
  36. Shattil SJ (1999) Signaling through platelet integrin  $\alpha_{IIb}\beta_3$ : inside-out, outside-in, and sideways. *Thromb Haemost* 82:318–325 [CrossRef](#) [PubMed](#) [Google Scholar](#)
  37. Kim C, Ye F, Ginsberg MH (2011) Regulation of integrin activation. *Annu Rev Cell Dev Biol* 27:321–345 [CrossRef](#) [PubMed](#) [Google Scholar](#)
  38. Grove J, Marsh M (2011) Host-pathogen interactions: the cell biology of receptor-mediated virus entry. *J Cell Biol* 195:1071–1082 [CrossRef](#) [PubMed](#) [PubMedCentral](#) [Google Scholar](#)
  39. Marsh M, Helenius A (2006) Virus entry: open sesame. *Cell* 124:729–740 [CrossRef](#) [PubMed](#) [Google Scholar](#)
  40. Bos JL (2005) Linking Rap to cell adhesion. *Curr Opin Cell Biol* 17:123–128 [CrossRef](#) [PubMed](#) [Google Scholar](#)
  41. Burridge K, Wennerberg K (2004) Rho and Rac take center stage. *Cell* 116:167–179 [CrossRef](#) [PubMed](#) [Google Scholar](#)
  42. Feng Y, Press B, Wandinger-Ness A (1995) Rab 7: an important regulator of late endocytic membrane traffic. *J Cell Biol* 131:1435–1452 [CrossRef](#) [PubMed](#) [Google Scholar](#)
  43. Shen B, Zhao X, O'Brien KA, Stojanovic-Terpo A, Delaney MK, Kim K, Cho J, Lam SC, Du X (2013) A directional switch of integrin signalling and a new anti-thrombotic strategy. *Nature* 503:131–135 [CrossRef](#) [PubMed](#) [PubMedCentral](#) [Google Scholar](#)
  44. Arachiche A, Mumaw MM, de la Fuente M, Nieman MT (2013) Protease-activated receptor 1 (PAR1) and PAR4 heterodimers are required for PAR1-enhanced cleavage of PAR4 by  $\alpha$ -thrombin. *J Biol Chem* 288:32553–32562 [CrossRef](#) [PubMed](#) [PubMedCentral](#) [Google Scholar](#)
  45. Coughlin SR (1999) How the protease thrombin talks to cells. *Proc Natl Acad Sci U S A* 96:11023–11027 [CrossRef](#) [PubMed](#) [PubMedCentral](#) [Google Scholar](#)
  46. Coughlin SR (2000) Thrombin signalling and protease-activated receptors. *Nature* 407:258–264 [CrossRef](#) [PubMed](#) [Google Scholar](#)
  47. Bilodeau ML, Hamm HE (2007) Regulation of protease-activated receptor (PAR) 1 and PAR4 signaling in human platelets by compartmentalized cyclic nucleotide actions. *J Pharmacol Exp Ther* 322:778–788 [CrossRef](#) [PubMed](#) [Google Scholar](#)
  48. Voss B, McLaughlin JN, Holinstat M, Zent R, Hamm HE (2007) PAR1, but not PAR4, activates human platelets through a  $G_{i/o}$ /phosphoinositide-3 kinase signaling axis. *Mol Pharmacol* 71:1399–1406 [CrossRef](#) [PubMed](#) [Google Scholar](#)
  49. McBane RD 2nd, Hassinger NL, Mruk JS, Grill DE, Chesebro JH (2005) Direct thrombin inhibitors are not equally effective in vivo against arterial thrombosis: in vivo evaluation of DuP714 and argatroban in a porcine angioplasty model and comparison to r-hirudin. *Thromb Res* 116:525–532 [CrossRef](#) [PubMed](#) [Google Scholar](#)
  50. Wen W, Young SE, Duvernay MT, Schulte ML, Nance KD, Melancon BJ, Engers J, Locuson CW 2nd, Wood MR, Daniels JS, Wu W, Lindsley CW, Hamm HE, Stauffer SR (2014) Substituted indoles as selective protease activated receptor 4 (PAR-4) antagonists: discovery and SAR of ML354. *Bioorg Med Chem Lett* 24:4708–4713 [CrossRef](#) [PubMed](#) [PubMedCentral](#) [Google Scholar](#)
  51. Diabate M, Munro P, Garcia E, Jacquet A, Michel G, Obba S, Gonçalves D, Luci C, Marchetti S, Demon D, Degos C, Bechah Y, Mege JL, Lamkanfi M, Auberger P, Gorvel JP, Stuart LM, Landraud L, Lemichez E, Boyer L (2015) *Escherichia coli*  $\alpha$ -hemolysin counteracts the anti-virulence innate immune response triggered by the Rho GTPase activating toxin CNF1 during bacteremia. *PLoS Pathog* 11:e1004732 [CrossRef](#) [PubMed](#) [PubMedCentral](#) [Google Scholar](#)
  52. Cheung AL, Bayer AS, Zhang G, Gresham H, Xiong YQ (2004) Regulation of virulence determinants in vitro and in vivo in *Staphylococcus aureus*. *FEMS Immunol Med Microbiol* 40:1–9 [CrossRef](#) [PubMed](#) [Google Scholar](#)
  53. Aktories K, Barbieri JT (2005) Bacterial cytotoxins: targeting eukaryotic switches. *Nat Rev Microbiol* 3:397–410 [CrossRef](#) [PubMed](#) [Google Scholar](#)
  54. Iliev AI, Djannatian JR, Nau R, Mitchell TJ, Wouters FS (2007) Cholesterol-dependent actin remodeling via RhoA and Rac1 activation by the *Streptococcus pneumoniae* toxin pneumolysin. *Proc Natl Acad Sci U S A* 104:2897–2902 [CrossRef](#) [PubMed](#) [PubMedCentral](#) [Google Scholar](#)

55. Nguyen CT, Le NT, Tran TD, Kim EH, Park SS, Luong TT, Chung KT, Pyo S, Rhee DK (2014) *Streptococcus pneumoniae* ClpL modulates adherence to A549 human lung cells through Rap1/Rac1 activation. Infect Immun 82:3802–3810 [CrossRef](#) [PubMed](#) [PubMedCentral](#) [Google Scholar](#)
56. Feistritzer C, Riewald M (2005) Endothelial barrier protection by activated protein C through PAR1-dependent sphingosine 1-phosphate receptor-1 crossactivation. Blood 105:3178–3184 [CrossRef](#) [PubMed](#) [Google Scholar](#)
57. Feistritzer C, Schuepbach RA, Mosnier LO, Bush LA, Di Cera E, Griffin JH, Riewald M (2006) Protective signaling by activated protein C is mechanistically linked to protein C activation on endothelial cells. J Biol Chem 281:20077–20084 [CrossRef](#) [PubMed](#) [Google Scholar](#)
58. Bae JS, Yang L, Manithody C, Rezaie AR (2007) The ligand occupancy of endothelial protein C receptor switches the protease-activated receptor 1-dependent signaling specificity of thrombin from a permeability-enhancing to a barrier-protective response in endothelial cells. Blood 110:3909–3916 [CrossRef](#) [PubMed](#) [PubMedCentral](#) [Google Scholar](#)

## MATERIALS TEXT

### 2.1 Microspheres, Supplies, and Equipment

1. Cyto-Plex™ far-red fluorescent carboxylated microspheres (beads), uniform 4–5 µm in diameter, 12 sets with 12 discrete dye levels, at 10<sup>8</sup> beads/mL, 1 mL of each set (Thermo Fisher Scientific): We use the 5.4 µm sized beads.
2. Carboxyl polystyrene beads, 5% w/v, 10 mL (Spherotech): Our batch was 5.28 µm.
3. Amino polystyrene beads, 5% w/v, 10 mL (Spherotech): Our batch was 3.57 µm.
4. Quantum™ FITC MESF (Molecules of Equivalent Soluble Fluorochrome) beads, five sets of commercial beads in which each subset is functionalized with discrete titers of fluorescein conjugates (Bangs Labs).
5. Refrigerated microcentrifuge with swinging bucket rotor and 0.65 mL microcentrifuge tubes.
6. Flow cytometer with a far-red laser, such as an Accuri C6.
7. pH meter.
8. Rotator, nutator.
9. Nitrogen-bubbling apparatus.

### 2.2 Synthesis of Glutathione Beads

1. 1% (v/v) Tween-20 stock.
2. pH 6 buffer: 0.1 M 2-(4-morpholino)-ethane sulfonic acid (MES), pH 6.0, 0.15 M NaCl, 0.01% (v/v) Tween-20.
3. 1-Ethyl-3-(dimethylaminopropyl) carbodiimide hydrochloride (EDAC).
4. Sulfo-N-hydroxysuccinimide (SNHS).
5. Rinse solution: 0.15 M NaCl, 0.01% (v/v) Tween-20, with no pH buffer.
6. pH 8.4 buffer: 0.1 M NaHCO<sub>3</sub>, pH 8.4, 0.01% (v/v) Tween-20.
7. 2 M 1,6-diaminohexane (hexamethylenediamine), pH 8.4.
8. pH 7 buffer: 0.1 M Sodium phosphate, pH 7.0, 0.01% (v/v) Tween-20.
9. Bifunctional crosslinker: 0.2 M Sulfosuccinimidyl 4-[N-maleimidomethyl] cyclohexane-1-carboxylate (sSMCC) in dimethyl sulfoxide (DMSO). Store at –80 °C.
10. 0.2 M Reduced glutathione, pH 7.0: Store in 50 µL aliquots at –20 °C.
11. 5 mg/mL Alexa Fluor 488 NHS ester (Thermo Fisher Scientific) in DMSO: Store at –80 °C
12. A fusion protein such as glutathione-S-transferase-green fluorescent protein (GST-GFP) to measure glutathione on the GST-functionalized beads, or your laboratory's GST fusion protein and a fluorescent detection agent that binds to it.

### 2.3 Cell Culture

The G-Trap assay is used to measure GTP loading of multiple GTPase targets, found in cell lysates [16, 17]. The reader may cultivate cells using applicable standard procedures for their target cells, and treat cells with known activators and inhibitors (see Table 1) [16, 17] to establish the applicability of the assay in the setting defined by the reader.

### 2.4 GST-Effector Protein Production

Following GST-effector chimeras are used for the studies described here:

1. p21 activated kinase protein-binding domain (PAK-1 PBD), a Rac1 effector (MilliporeSigma).
2. Raf-1 (v-raf-1 murine leukemia viral oncogene homolog 1) RBD, a Ras effector protein (MilliporeSigma).
3. Rhotekin-RBD, a Rho effector protein (Cytoskeleton).
4. Ral-GDS RBD, a Rap-1 effector protein (Thermo Fisher Scientific).
5. GST-RILP, prepared as previously described [16].

### 2.5 GTPase Assay



1. Antibodies: Monoclonal rabbit anti-Rap1 (Santa Cruz Biotechnology); monoclonal mouse antibodies anti-Rho (A, B, C) clone 55, anti-Rac1, anti-Rab7, and the secondary antibody goat anti-mouse IgG (H + L) conjugated to Alexa Fluor 488 (MilliporeSigma); monoclonal mouse anti-Ras antibody (Abcam).
2. Activators and inhibitors: Rap1 activator 8-Cpt-2me-cAMP (50  $\mu$ M) (R&D Systems); Rac1 inhibitor NSC23766 (100  $\mu$ M) and Rho activator calpeptin (1  $\mu$ M) (MilliporeSigma); recombinant epidermal growth factor (EGF) (10 nM) (Thermo Fisher Scientific); mP6, a myristoylated hexapeptide (myr-FEERA-OH), custom synthesized at New England Peptide, H-Ras and K-Ras inhibitor, FTI 277 (100 nM) (Tocris); Rap1 inhibitor (GGTI 298) (10  $\mu$ M).
3. 2 $\times$  RIPA buffer: 100 mM Tris-HCl, pH 7.4, 300 mM NaCl, 2 mM ethylenediaminetetraacetic acid (EDTA), 2 mM NaF, 2 mM  $\text{Na}_3\text{VO}_4$ , 2% (v/v) NP-40, 0.5% (w/v) sodium deoxycholate. Just before adding to the culture medium supplement with 2 mM phenylmethylsulfonyl fluoride (PMSF) and 2 $\times$  protease inhibitors (Halt<sup>™</sup> Protease and Phosphatase Cocktail # 78442, ThermoScientific).
4. HHB buffer: 7.98 g/L HEPES (Na salt), 6.43 g/L NaCl, 0.75 g/L KCl, 0.095 g/L  $\text{MgCl}_2$ , and 1.802 g/L glucose.
5. HPSMT buffer (an intracellular mimic): 30 mM HEPES, pH 7.4, 140 mM KCl, 12 mM NaCl, 0.8 mM  $\text{MgCl}_2$ , 0.01% (v/v) Tween-20.
6. Blocking buffer 1: 0.1% Bovine serum albumin (BSA) in HPSMT.
7. Blocking buffer 2: 5% BSA in HPSMT.
8. 10 mM EDTA and 0.2% sodium azide for use at 1:10 dilution in storage buffer.

#### SAFETY WARNINGS



Please refer to Safety Data Sheets (SDS) for health and environmental hazards.

### 3.1 Synthesis of Glutathione Beads




2h 6m

1

High-site-density glutathione-derivatized beads used for flow cytometry have been synthesized previously from 13  $\mu$ m dextran-cross-linked agarose beads [26, 27], and 4  $\mu$ m amino polystyrene beads [20]. In this method, 5.4  $\mu$ m Cyto-Plex<sup>™</sup> carboxylated polystyrene bead sets are first converted to amino beads, and then to glutathione beads. We use standard practices with high concentrations of reagents to obtain a high glutathione site density on the beads. A high surface coverage of glutathione (GSH) enables robust capture of soluble GST fusion proteins [28]. The 12 Cyto-Plex<sup>™</sup> carboxyl bead sets are coded with 12 graded intensities of far-red fluorescence when excited at a fixed wavelength, which does not interfere with fluorescein or phycoerythrin fluorescence detection. We suggest the use of a centrifuge with a swinging-bucket rotor and slow deceleration for ease of removing 90% of the supernatant, without disturbing the beads, during the many centrifugations in this synthesis. All reactions are at room temperature. While the protocol below is written for Cyto-Plex<sup>™</sup> beads, we used an inexpensive (nonfluorescent) set of polystyrene carboxyl beads for pilot-testing our protocol for optimizing the synthetic conversion of carboxyl- to amino-functional groups on the beads, and subsequent coupling to glutathione (*see Note 1*).



- 2 A bead set in its bottle is rocked gently on its side for  **00:02:00**, rotated  $\frac{1}{4}$  turn and rocked again for  **00:02:00**<sup>4m</sup>, and continued until the beads are in a milky suspension. 15 s of immersion in a low-power ultrasonic bath can help the resuspension.

3  


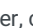
Place  **4  $\mu$ l 1% Tween-20** in a 0.65 mL centrifuge tube, add  **400  $\mu$ l bead suspension**, mix gently with a pipette, and then allow the suspension to settle  **Overnight** to coat the beads and the tube with Tween-20, decreasing bead aggregation and adhesion to the tube (*see Note 2*).

4 

Remove all but ~10 µL of the supernatant, resuspend the beads, and give two standard washes:

- 4.1 For a regular wash, add  **100 µl pH 6 buffer** to 10 µL of suspension, mix with a vortex mixer, centrifuge at  **5000 x g, 00:02:00** , (between 3,000-5,000 x g) , remove 100 µL of supernatant, and resuspend the remaining 10 µL of beads with a vortex mixer.





This standard wash assures that a nominal factor of 10× dilution of the undesired solute is achieved. Resuspension in minimal buffer ensures equal exposure of all beads to the next reagent.

- 4.2 Repeat the wash: For a regular wash, add  **100 µl pH 6 buffer** to 10 µL of suspension, mix with a vortex mixer, centrifuge at  **5000 x g, 00:02:00** , (between 3,000-5,000 x g) , remove 100 µL of supernatant, and resuspend the remaining 10 µL of beads with a vortex mixer.

This standard wash assures that a nominal factor of 10× dilution of the undesired solute is achieved. Resuspension in minimal buffer ensures equal exposure of all beads to the next reagent.

5 

30m





Weigh  **4 mg EDAC** and  **8 mg sNHS** into a microfuge tube, add  **100 µl pH 6 buffer** , immediately dissolve by vortexing, add this to a bead set, and mix. Place the microfuge tube in a rotator with a horizontal axis of rotation for  **00:30:00** to keep the beads in suspension, away from the tube lid and sides, while the site density of sNHS ester intermediate builds on the beads.

6  

Centrifuge at  **5000 x g, 00:02:00** , (between 3,000-5,000 x g) , remove all but 10 µL of the supernatant, resuspend the beads, and then wash two times with  **100 µl rinse solution** , which will dilute the EDAC and sNHS while keeping the pH low and the sNHS ester intact.

7  

30m

Resuspend the beads in  **180 µl pH 8.4 buffer** , immediately add  **20 µl 2 M 1,6 diaminohexane** , mix, and rotate as in **step 5** (place the microfuge tube in a rotator with a horizontal axis of rotation) for  **00:30:00** .  
Centrifuge at  **3000 x g, 00:02:00** , remove all but 10 µL of supernatant, and resuspend the beads.

8 

Wash four times with pH 8.4 buffer and resuspend the amino beads into a total of 90 µL of pH 8.4 buffer:

- 8.1 (Wash 1/4): Wash with pH 8.4 buffer.

8.2 (Wash 2/4): Wash with pH 8.4 buffer.

8.3 (Wash 3/4): Wash with pH 8.4 buffer.

8.4 (Wash 4/4): Wash with pH 8.4 buffer.

8.5 Resuspend the amino beads into a total of **90 µl pH 8.4 buffer**.

8.6 

We derivatize six sets of beads at a time and leave the six sets **Overnight** at this stage. The amino site density can be measured in a pilot assay to ensure optimal conversion of carboxyl- to amino-terminal groups (*see* **Note 3**).

9 

30m

Add **10 µl 200 mM sSMCC in DMSO**, mix, rotate as in **step 5** (place the microfuge tube in a rotator with a horizontal axis of rotation) for **00:30:00** while the site density of the crosslinker's maleimide builds on the beads, centrifuge, and resuspend the beads in **10 µl**.

10 

Wash with **100 µl pH 7 buffer** and resuspend to **360 µl pH 7 buffer**.

11 Prepare and test the nitrogen-bubbling apparatus to give a slow series of bubbles (*see* **Note 4**).

12 Add **2 µl 100 mM EDTA** and **20 µl 200 mM glutathione, pH 7** and bubble nitrogen slowly through the suspension for **00:02:00** to remove most of the oxygen. Cap the tube and rotate it slowly for **00:30:00**.<sup>32m</sup>

13 

Centrifuge at **3000 x g, 00:02:00**, remove all but 10 µL of supernatant, and resuspend the glutathione beads.

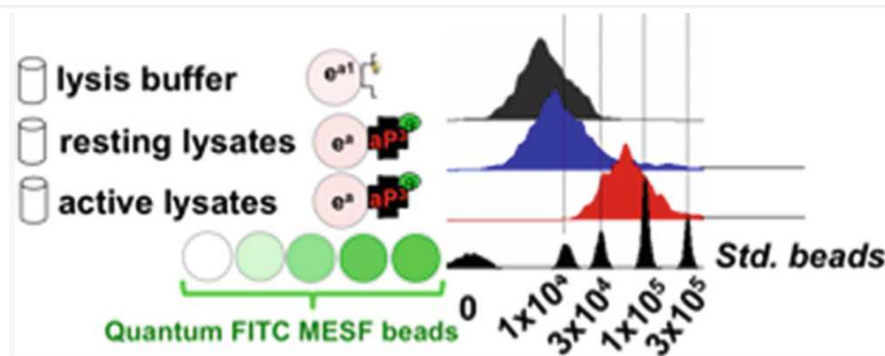
Wash beads four times in the storage buffer of your choice, reducing the concentration of glutathione from 20 mM to below 2 µM:

- 13.1 (Wash 1/4): Wash beads in the storage buffer of your choice (reducing the concentration of glutathione from 20 mM to below 2  $\mu$ M).
- 13.2 (Wash 2/4): Wash beads in the storage buffer of your choice (reducing the concentration of glutathione from 20 mM to below 2  $\mu$ M).
- 13.3 (Wash 3/4): Wash beads in the storage buffer of your choice (reducing the concentration of glutathione from 20 mM to below 2  $\mu$ M).
- 13.4 (Wash 4/4): Wash beads in the storage buffer of your choice (reducing the concentration of glutathione from 20 mM to below 2  $\mu$ M).

## 14

Add **1 mM EDTA** and **0.02 % (w/v) sodium azide** in the storage buffer to inhibit bacterial growth. Store at **4 °C** at a concentration of  $10^8$  beads/mL. The beads have been stable for over 2 years. A portion of each bead set is diluted  $10\times$  in a storage buffer for ease of assay. Each assay uses  $10^4$  beads per target GTPase or 1  $\mu$ L of diluted beads.

It is useful to quantify the number of GST-binding sites on the newly functionalized beads using commercial Quantum™ FITC MESF (see Fig. 2) or other methods [29, 30]. Assay the beads by incubating them in 25 nM GST-GFP for 30 min. Use 100  $\mu$ M soluble glutathione to determine nonspecific binding of GST-GFP to the glutathione beads. Using Quantum™ FITC MESF beads, the glutathione beads synthesized as described support >1.0 million GST-binding sites. At high surface density (>1300 fluorophores/ $\mu\text{m}^2$ ), fluorophores on a bead surface undergo self-quenching with increasing site occupancy [31]. It is therefore likely that the 1.0 million sites determined by the calibration beads are a lower limit. However, this measure is useful for tracking the useful shelf life of the beads.



**Fig. 2**  
Single-analyte assay for RILP: GTP-Rab7 captured on beads. Fluorescently labeled detection antibody added to lysis buffer is used to assess nonspecific binding of the antibody to beads. Flow cytometry histograms of RILP-RBD effector beads incubated at 4 °C with resting HeLa cell lysates or with EGF-stimulated HeLa cell lysates show increased Rab7-GTP bound, the levels of which can be quantified using commercial standard calibration beads (Quantum™ FITC MESF). Quantum™ FITC MESF beads comprise five sets of distinct bead populations. Each bead population is distinguished by a discrete number of doped fluorophores of known calibration. The average fluorophores/bead on each bead population is shown on the x-axis. The calibration beads are used to quantify the occupancy of Rab7-specific antibodies on RILP-effector beads. After correcting for nonspecific binding,  $7.1 \pm 1.2 \times 10^3$  Rab7-GTP molecules/bead were recovered in resting cell lysates, and  $6.7 \pm 0.3 \times 10^4$  Rab7-GTP molecules/bead were retrieved in EGF-stimulated cell lysates [16]

